Journal of Dentistry 166 (2026) 106352

Contents lists available at ScienceDirect

Journal of Dentistry

journal homepage: www.elsevier.com/locate/jdent

A comparative evaluation of Vat-photopolymerization and PolyJet 3D printers using multiple measurement methods

Márton József Suta [a], Attila Csík [b], Sándor Bodzás [c], Dániel Nemes [c,d], Gábor Balogh [c], Mónika Béresová [e], Sándor Manó [f], Loránd Csámer [f], József Mihály Gáll [g], Igor R. Blum [h], Csaba Hegedűs [a,*]

[a] Department of Biomaterials and Prosthetic Dentistry, Faculty of Dentistry, University of Debrecen, Debrecen, Hungary, aDoctoral School of Dental Sciences, Doctoral Council of Medical Sciences, University of Debrecen, Debrecen, Hungary
[b] HUN-REN Institute for Nuclear Research, Debrecen, Hungary
[c] Department of Mechanical Engineering, Faculty of Engineering, University of Debrecen, Debrecen, Hungary
[d] Doctoral School of Informatics, University of Debrecen, Debrecen, Hungary
[e] Department of Medical Imaging, Faculty of Medicine, University of Debrecen, Debrecen, Hungary
[f] Laboratory of Biomechanics, Faculty of Medicine, Department of Orthopaedic Surgery, University of Debrecen, Debrecen, Hungary
[g] Department of Applied Mathematics and Probability Theory, Faculty of Informatics, University of Debrecen, Debrecen, Hungary
[h] Faculty of Dentistry, Oral & Craniofacial Sciences, King's College London, London, United Kingdom

ARTICLE INFO

Keywords:
3D printing
Distortion measurement
microCT
PolyJet
Stereolithography

ABSTRACT

Objective: Given the widespread adoption of additive manufacturing in dentistry, assessing the dimensional accuracy of printed objects is critical. This study aimed to evaluate the three-dimensional (3D) deviations produced by four printers utilizing SLA, mSLA, and PolyJet technologies, employing three distinct measurement methodologies.
Materials and method: Sixty cube specimens with a 15 mm edge length were fabricated ($n = 15$ per group) using four different 3D printers: Form 3B+, Prusa SL1, Objet 30 Orthodesk and Connex 260. The distance between opposing cube faces was assessed at twelve predefined locations using three measurement methodologies: manual measurement with a digital micrometer, a micro-computed tomography (micro-CT) system, and an optical scanner.
Results: Micro-CT and micrometer measurements yielded reliable dimensional data, whereas the optical scanner consistently yielded underestimated values. Micro-CT yielded superior definition of the specimen surface topography Mean micro-CT measurements differed significantly from the nominal reference value (15,000 μm) in 15 of 16 instances for X coordinates ($p < 0.01$), 15 instances for Y coordinates ($p < 0.015$), and in 12 instances for Z coordinates ($p < 0.03$). Deviations were significantly higher in the X and Y axes compared to the Z axis.
Conclusions: Micro-CT was identified as the most precise measurement method among those evaluated. Of the printers tested, the Connex260 demonstrated superior overall performance, exhibiting the lowest dimensional deviation. Across all devices, the highest accuracy was consistently observed along the Z-axis.
Clinical significance: Even minor dimensional inaccuracies in additively manufactured components can compromise the fit, marginal integrity, and function of restorations, directly impacting patient comfort and treatment longevity. Consequently, the careful selection of appropriate printing technologies, validated by precise measurement protocols, is critical for ensuring predictable clinical outcomes.

1. Introduction

The term '3D printing' is frequently used synonymously with 'additive manufacturing' (AM) and 'rapid prototyping' (RP) . It describes the process of fabricating three-dimensional objects layer-by-layer based on computer-aided design (CAD) data [1,2]. Within dentistry, this technology facilitates a broad spectrum of applications, ranging from the production of custom trays, working models, and surgical guides to

* Corresponding author.
E-mail address: hegedus.csaba.prof@dental.unideb.hu (C. Hegedűs).

https://doi.org/10.1016/j.jdent.2026.106352
Received 22 December 2025; Accepted 9 January 2026
Available online 10 January 2026

complete dentures and biodegradable scaffolds [2,3]. According to the International Organization for Standardization standard document ISO/ASTM 52,900:2021 standard, AM processes are classified into seven distinct categories: binder jetting, directed energy deposition, material extrusion, material jetting, powder-bed fusion, sheet lamination, and Vat Photopolymerization (VPP) [4,5]. Among these categories, VPP is one of the most established and widely applied techniques [6]. This category includes Stereolithography (SLA) and masked stereolithography apparatus (mSLA), both of which employ ultraviolet (UV) light to selectively polymerize and cure liquid resin layer-by-layer [1,5,7]. In contrast, PolyJet technology falls under the material jetting category, depositing droplets of photopolymer onto a build platform, that are subsequently cured by a UV light source [5,6].

Despite these advancements, the final 3D-printed part often deviates from the original CAD design due to the intrinsic limitations of additive manufacturing (AM) [8]. However, there is currently limited evidence in the literature comparing the accuracy and reliability of manual micrometer measurements, micro-CT, and optical scanning when evaluating these three-dimensional distortions across different printing technologies. One of the key challenges of 3D printing is distortion, which may arise from multiple interacting factors [8]. Beyond technical, engineering, informational, and manufacturing limitations [2,8,9], the initiation and termination of the polymer-level reactions at the molecular level have also been identified as potential sources of inaccuracy [10,11]. A recent review further highlighted that the main challenges of AM in biomedical applications include material selection, dimensional accuracy, consistency of quality, regulatory compliance, cost-effectiveness, quality control, and the lack of standardization [9]. Therefore, evaluating dimensional accuracy across diverse AM technologies is essential for determining their clinical suitability. The aim of this study was to assess and compare the three-dimensional deviations of specimens fabricated using four 3D printers (SLA, mSLA, and PolyJet), as quantified by three distinct measurement methodologies. The null hypotheses tested were: (1) that no significant statistical differences would be observed among the three measurement methodologies; and (2) that no significant differences in volumetric deviation would be present across the X, Y, and Z axes of the 3D-printed specimens.

2. Materials and methods

2.1. Specimen design

A cube specimen, with a 15 mm edge length was designed using SolidWorks 3D CAD software (Dassault Systèmes SolidWorks, Waltham, MA, USA) (Fig. 1). An integrated handle was incorporated into the design to facilitate handling during post-processing procedures. In total, sixty cube specimens were fabricated. The digital specimens were exported in Standard Tessellation Language (STL) format for subsequent fabrication.

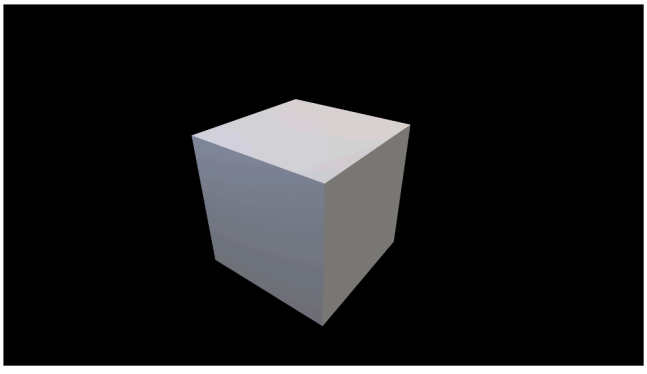

Fig. 1. Digital reference model of the 15 mm cube specimen.

2.2. 3D printing protocols

The STL file was prepared for fabrication using four different additive manufacturing systems. The technical specifications, printing materials, and manufacturer details for each device are presented in Table 1. Fifteen specimens were manufactured for each group ($n = 15$) using the minimum layer thickness supported by each printer. To ensure comparability across groups, a standardized build orientation was maintained for all specimens.

2.3. Post-processing

All printed specimens were subjected to post-processing strictly in accordance with the respective manufacturers' instructions. These procedures consistently included solvent cleaning to remove residual uncured resin and subsequent post-curing, alongside any specific additional measures mandated for each material type.

2.4. Measurement methods

The specimens featured a cubic geometry; the integrated handle served solely for fixation and manipulation and was strictly excluded from all dimensional analyses. For each specimen ($n = 15$ per group, $N = 60$ in total), the linear distance between opposing faces was quantified at twelve standardized reference points using all three measurement methodologies. An overview of the experimental workflow is shown in Fig. 2.

2.4.1. Digital micrometer measurement

Dimensional accuracy was first assessed using a high-precision digital micrometre [12,13]. For each specimen, the linear distance between opposing faces was recorded at the twelve predefined coordinates (Fig. 3). This technique was selected to serve as the baseline contact-measurement method, representing a widely accessible and cost-effective clinical reference standard.

2.4.2. Micro-computed tomography (micro-CT)

Each specimen was digitized using a high-resolution micro-CT system (SkyScan 1272, Bruker Corp., Billerica, MA, USA). Scans were performed at 60 kV and 160 μA for Connex 260, Objet 30 and Prusa SL1 groups and at 100 kV and 100 μA for Form 3B+ specimens with an isotropic voxel size of 13 μm. Following 3D volumetric reconstruction, the data allowed for the precise determination of linear distances between opposing faces. Measurements were extracted from the digital volume at the same twelve corresponding coordinates used in the micrometer analysis, providing a high-precision, non-contact assessment of surface morphology and dimensional fidelity.

2.4.3. Optical scanning system

Digital surface models of the specimens were acquired using an optical scanning system (Atos Core 200 optical scanner, Carl Zeiss GOM Metrology GmbH, Braunschweig, Germany). Following digitization, linear measurements were computed from the resulting STL meshes the same twelve corresponding coordinates used in the previous methodologies. Given prior reports indicating that optical scanning may underestimate specific dimensions [14,15], this potential systematic bias was critically factored into the comparative data analysis.

2.4.4. Measurement repeatability

To evaluate the precision of the methodologies, a single specimen was randomly selected from the total cohort ($N = 60$). The linear dimensions (X1, Y1, and Z1) between opposing faces were measured fifteen consecutive times using each of the three measurement systems. Levene's test was subsequently employed to compare the standard deviations across the groups, thereby assessing the homogeneity of variance and the relative reliability of each method.

Table 1
Specifications of the 3D printers and materials utilized in the study.

3D printer	Technology	Material	Layer thickness	Post-processing
Form3B+ (Formlabs Inc., Sommerville, USA)	Stereolithography	Temporary CB A2 (Formlabs Inc., Sommerville, USA)	50 μm	Wash in isopropyl alcohol (IPA) for 3 min, dry, cure at 60 °C and 405 nm LED wavelength for 20 min.
Prusa SL1 (Prusa Research a.s., Prague, Czech Republic)	Masked Stereolithography	Clear Biocompatible MED610 (Stratasys Ltd., Rehovot, Israel)	50 μm	Wash in isopropyl alcohol (IPA) for 3 min, dry, and cure with 405 nm LED wavelength for 3 min.
Objet 30 Orthodesk (Stratasys Ltd., Rehovot, Israel)	PolyJet	Biocompatible VeroGlaze MED 620 (Stratasys Ltd., Rehovot, Israel) SUP 705 support material (Stratasys Ltd., Rehovot, Israel)	28 μm	Support SUP705 removal with waterjet Soak for 3 h in a 1-percent solution of sodium hydroxide, rinse Soak for 30 min in isopropyl alcohol (IPA), dry.
Connex 260 (Stratasys Ltd., Rehovot, Israel)	PolyJet	Clear Biocompatible MED610 (Stratasys Ltd., Rehovot, Israel) SUP 705 support material (Stratasys Ltd., Rehovot, Israel)	16 μm	Support SUP705 removal with waterjet Soak for 3 h in a 1-percent solution of sodium hydroxide, rinse Soak for 30 min in isopropyl alcohol (IPA), dry.

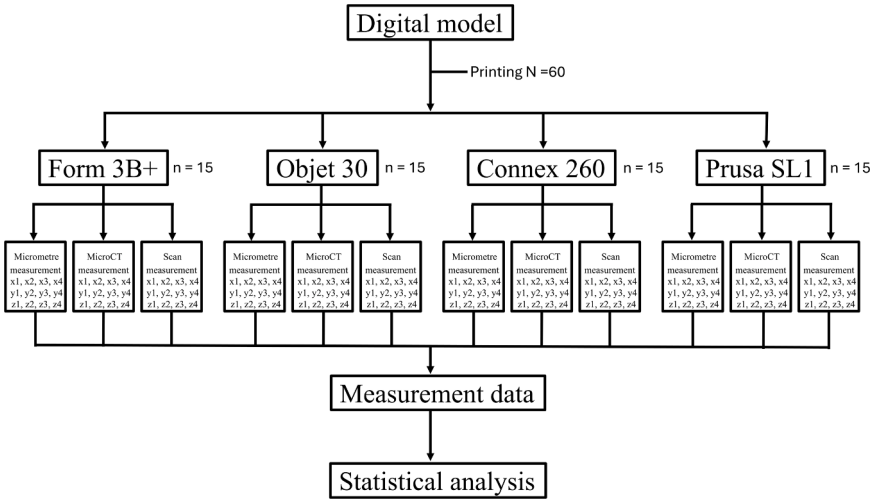

Fig. 2. Flowchart illustrating the experimental procedure.

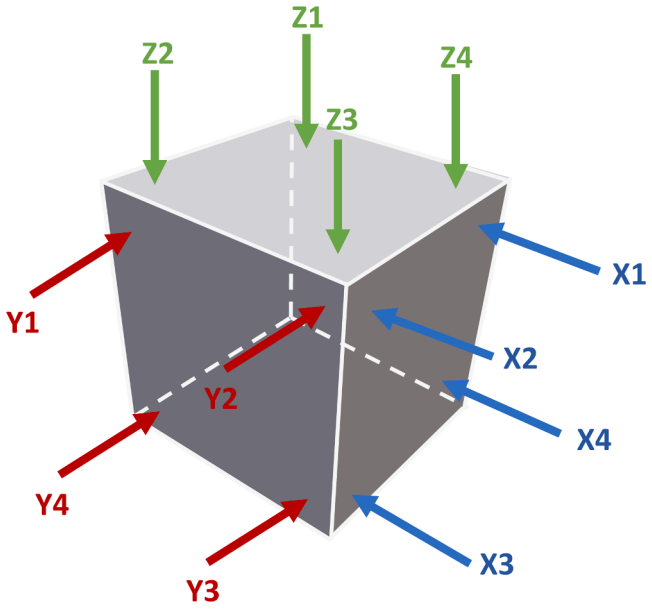

Fig. 3. Schematic representation of the test specimen indicating the twelve standardized reference points used for dimensional measurement.

2.4.5. Digital micrometer protocol

Measurements were performed by a single operator (MJS) using an Absolute Digimatic Quickmike Series 227 micrometre (Mitutoyo Corp., Kawasaki, Japan). The instrument features a digital resolution of 1 μm and maximum permissible error of ± 2 μm. The measurement spindle has a diameter of 6.35 mm, creating a contact surface area of approximately 31.67 mm^2. Consequently, each recorded value represents the dimension at the most protruding point within this contact zone.

2.4.6. Micro-CT measurement

Specimens were digitized using a SkyScan 1272 micro-CT system (Bruker Corp., Billerica, MA, USA) at an image pixel resolution of 13 μm (1344 × 2016 matrix). For the Connex 260, Objet 30, and Prusa SL1 groups, acquisition settings were established at 60 kV and 160 μA utilizing a 0.25 mm aluminum filter. Conversely, the Form 3B+ specimens required a harder beam profile, utilizing 100 kV and 100 μA with a 0.11 mm copper filter. Following acquisition with standard geometrical corrections, projection images were reconstructed using SkyScan NRecon package (Version: 2.0.4.2). The reconstruction pipeline included algorithms for misalignment compensation, ring artifact removal, beam-hardening correction, and smoothing. Final measurements were executed in CTAn software (Bruker Corp., Billerica, MA, USA) on the reconstructed BMP/DICOM stacks.

2.4.7. Optical scan acquisition (Scan)

Three-dimensional surface acquisition was performed using an Atos Core 200 optical scanner (Carl Zeiss GOM Metrology GmbH, Braunchschweig, Germany) mounted on a Foba Alfae tripod (Foba AG, Wettswil am Albis, Switzerland). This methodology is hereafter referred to as "Scan". To facilitate accurate spatial registration, the specimens

were secured within a custom modular fixture constructed from the Alufix Classic 1 basic set (Witte Barskamp GmbH & Co. KG, Bleckede, Germany). Reference markers (1.5 mm medium-adhesion reference points; Carl Zeiss GOM Metrology GmbH, Braunschweig, Germany) were applied to the fixture in a stochastic pattern. These reference points, moving in unison with the specimen, ensured consistent alignment of the point clouds during capture. To optimize workflow efficiency and reproducibility, the fixture was mounted on an automated rotation unit (GOM Rot 360; Carl Zeiss GOM Metrology GmbH, Braunschweig, Germany). As the acquisition relied on structured light fringe projection, maintaining high contrast was essential. Optical surface properties such as glare, transparency, and light absorption were identified as potential sources of error. To mitigate these artifacts in the Connex 260 and Prusa SL1 groups, a uniform matte white coating was applied using Aesub Blue evaporating spray (Scanningspray Vertriebs GmbH, Dortmund, Germany), in accordance with the scanner manufacturer's guidelines. This coating introduced a known surface offset of 8–15 μm.

2.4.8. Data processing

Scan data were processed using GOM Inspect Suite 2020 software (Carl Zeiss GOM Metrology GmbH, Braunschweig, Germany), which performed automatic calibration adjustments based on ambient laboratory temperature The system operated with a point spacing (resolution) of 80 μm. On the resulting 3D meshes, the lengths of the twelve cube edges were quantified using the same protocol described for the previous methodologies.

2.5. Scanning electron microscope (SEM) analysis

Surface morphology was examined using a Thermo Scios 2 DualBeam system scanning electron microscope (Thermo Fisher Scientific, Waltham, MA, USA). Images were acquired at an accelerating voltage of 2 kV to maximize resolution while minimizing charging effects on the resin surfaces. Imaging was performed at magnifications of 80 × .

2.6. Statistical analysis

Descriptive statistics were calculated for each printer group and measurement methodology. To evaluate the accuracy of the printed specimens, a one-sample *t*-test was used to compare individual measurements against the nominal reference value (15,000 μm). The comparative performance of the three measurement methodologies was assessed using paired-sample *t*-tests. All statistical analyses were performed using IBM SPSS Statistics (Version 28.0.1.0, IBM Corp., Armonk, NY, USA), with the level of significance set at α=0.05. Data visualization, including boxplot generation, was conducted in R software (The R Foundation for Statistical Computing, Vienna, Austria) utilizing the ggplot2 package [16].

3. Results

Analysis of measurement repeatability revealed that the optical scanning method ("Scan") exhibited significantly higher standard deviations across all axes compared to the other methodologies, indicating lower precision. Conversely, micro-CT demonstrated the lowest standard deviations for two of the three axes, outperforming the digital micrometer (Table 2). Consequently, due to its superior precision and ability to capture detailed surface morphology, the micro-CT dataset was designated as the primary reference for the subsequent comparative analyses.

The measurement results for the specimens from all four printer groups are presented in Figs. 4–7. These images reveal that each printing process produced distinct surface topographies. Among the imaging modalities, Scanning Electron Microscopy (SEM) provided the superior visualization of surface morphology capturing the finest details. Micro-CT also offered high detail, though the voxel-based reconstruction introduced discrete stepwise transitions (aliasing) in the visual data. In contrast, the optical scanner tended to obscure fine surface details in its default mode; this setting was necessary, as higher-resolution capture protocols resulted in excessive image noise.

Table 2
Summary of measurement repeatability for the Micrometer, Micro-CT, and Scan methods (Mean ± Standard Deviation).

Method		X1	Y1	Z1
Micrometre	N	15	15	15
	Mean	15,116.6667	15,173.6000	14,948.7333
	Std. Deviation	7.96122	3.04256	6.07650
Micro-CT	N	15	15	15
	Mean	15,086.0667	15,136.3333	14,951.7333
	Std. Deviation	6.71317	6.34335	4.57426
Scan	N	15	15	15
	Mean	15,014.0667	15,095.4667	14,961.6667
	Std. Deviation	21.65135	36.96884	16.41283
Total	N	45	45	45
	Mean	15,072.2667	15,135.1333	14,954.0444
	Std. Deviation	45.55636	38.62559	11.63450

Figs. 8–10 present boxplots comparing the dimensional distributions obtained from the three different measurement methodologies (Micrometre, Micro-CT, and Scan). To provide a granular analysis, each figure visualizes data from 48 distinct experimental conditions, corresponding to the twelve specific measurement locations assessed across each of the four printer groups.

The comparison of measurement methods reveals a significant difference in the mean values for all X, Y and Z coordinates when assessed by micro-CT, micrometre and optical scan ($p < 0.01$), with the exception of coordinate X1, where no significant difference was found between microCT and micrometre. For the cases exhibiting statistically significant differences, the mean difference between micro-CT and micrometer measurements ranged from −80.5 μm to −22.7 μm. Comparisons between microCT and scan, as well as micrometre and scan, demonstrated significant mean differences ($p < 0.01$), ranging from +51.8 μm to +308.0 μm and from +90.2 μm to +377.2 μm, respectively. Descriptive statistics for the micro-CT measurements are presented in Table 3.

The comparison of micro-CT measurements against the nominal reference value (15,000 μm) yielded the following findings:

X-Axis: Significant dimensional deviations were observed in 15 of 16 cases ($P < 0.01$), with the singular excption of coordinate X2 for the Form 3B+.

Y-Axis: Similarly, 15 of 16 cases demonstrated significant differences ($P < 0.015$), with coordinate Y1 for the Form 3B+ representing the sole exception.

Z-Axis: Measurements along the Z-axis exhibited lower overall deviation compared to the X and Y planes. In this dimension, 12 instances showed significant differences ($P < 0.03$); the non-significant results were notably observed within the Objet30 printer group.

The comparison of mean printed values against the nominal reference value (15,000 μm), derived from the micro-CT dataset is shown in Table 4. The analysis included 15 specimens per printer, with four specific measurement locations assessed for each coordinate. In the table, the column ‘Significant cases’ denotes the number of locations (out of four), that exhibited a statistically significant difference from the nominal reference value target dimension (one-sample *t*-test; α=0.05). Correspondingly, the ”Difference” column quantifies the magnitude and direction of the deviation for these significant instances, strictly adhering to the specified notation scheme.

4. Discussion

Additive manufacturing technologies have been increasingly adopted in both industrial and dental domains. However, the heterogeneity in specimen and measurement methodologies across the literature

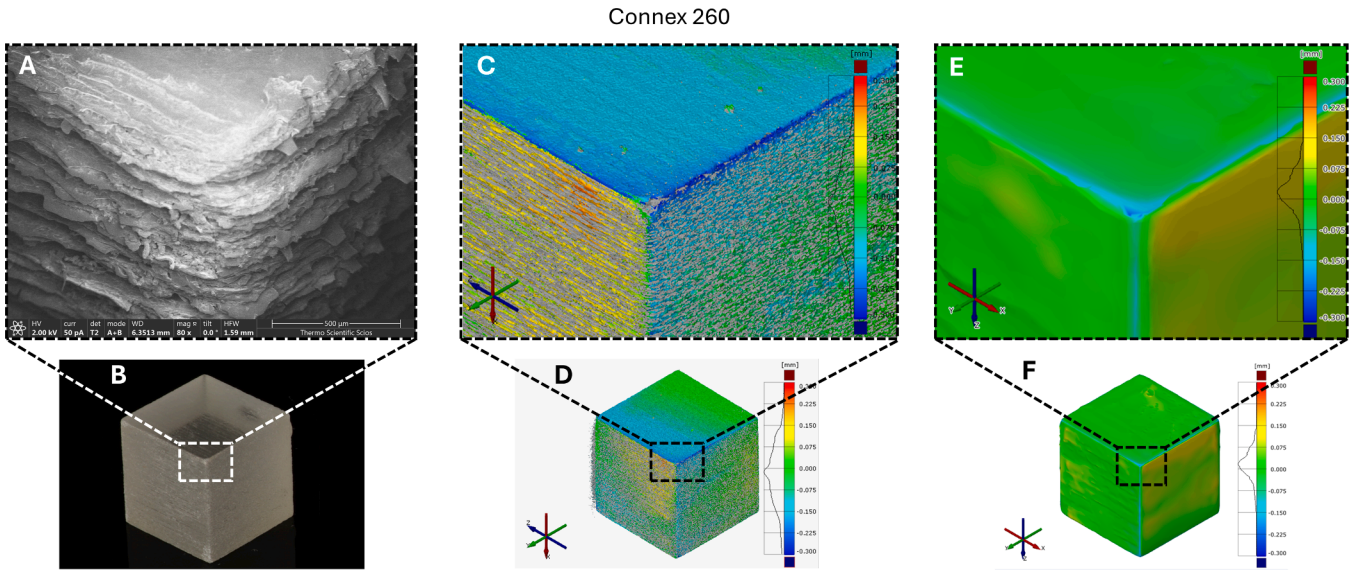

Fig. 4. Analysis of the Connex260 specimen. (A) Scanning electron micrograph (SEM) showing surface topography (original magnification 80 ×). (B) Macroscopic digital photograph of the printed specimen. (D) Color-coded deviation map (GOM Inspect Suite 2020) comparing the reference CAD model against the micro-CT reconstruction. (C) Close-up view of the cube vertex (corner) from the micro-CT comparison. (F) Deviation map comparing the reference CAD model against the optical scan (Atos Core 200). (E) Close-up view of the vertex from the optical scan comparison.

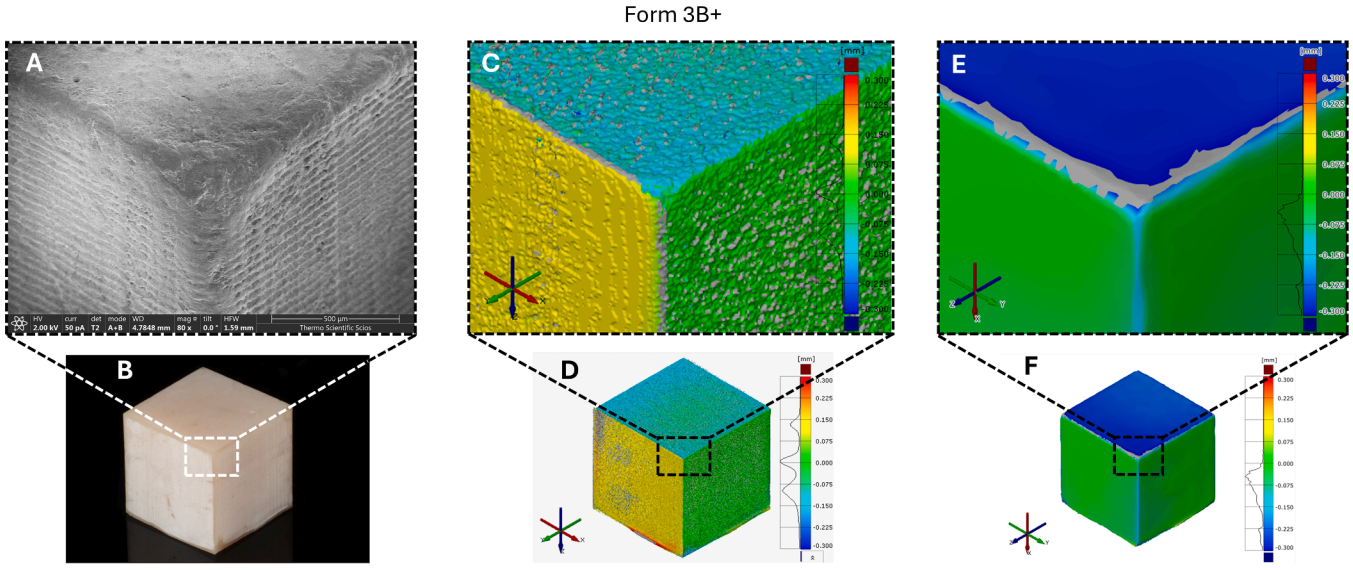

Fig. 5. Analysis of the Form 3B+ specimen. (A) Scanning electron micrograph (SEM) showing surface topography (original magnification 80 ×). (B) Macroscopic digital photograph of the printed specimen. (D) Color-coded deviation map (GOM Inspect Suite 2020) comparing the reference CAD model against the micro-CT reconstruction. (C) Close-up view of the cube vertex (corner) from the micro-CT comparison. (F) Deviation map comparing the reference CAD model against the optical scan (Atos Core 200). (E) Close-up view of the vertex from the optical scan comparison.

hampers direct comparison of results. Furthermore, there is a notable scarcity of data regarding the specific surface characteristics of 3D-printed objects, despite the fact that parameters such as smoothness, edge definition, and surface roundness are critical for prosthodontic success. To address this, the present study employed scanning electron microscopy at a low accelerating voltage (2 kV). This technique enabled the detailed, high-resolution assessment of surface morphology on insulating resin samples without the need for conductive gold coating, thereby preserving the original surface state. While manufacturers provide general design guidelines [17,18], and several previous studies have attempted to utilize standardised specimens [13,19,20] or ISO protocols [21–23], direct extrapolation of these findings to complex clinical applications - such as complete dentures - warrants caution. Furthermore, the selection of measurement methodology introduces significant variability. As illustrated in Fig. 11, a micrometer quantifies the outer envelope defined by the most prominent surface peaks. In contrast, micro-CT allows for the assessment of intricate internal structures, though the resulting measurements remain sensitive to technique-dependent factors, such as the precise definition of start and end points.

The limited resolving power of optical systems raises critical questions regarding their capacity to capture fine surface details and the subsequent reliability of algorithmic scan alignment. While superimposition and best-fit alignment techniques are widely employed [1,24,25], their accuracy is variable. Wan et al. demonstrated that these digital methods are highly reliable for assessing volume loss on flat surfaces

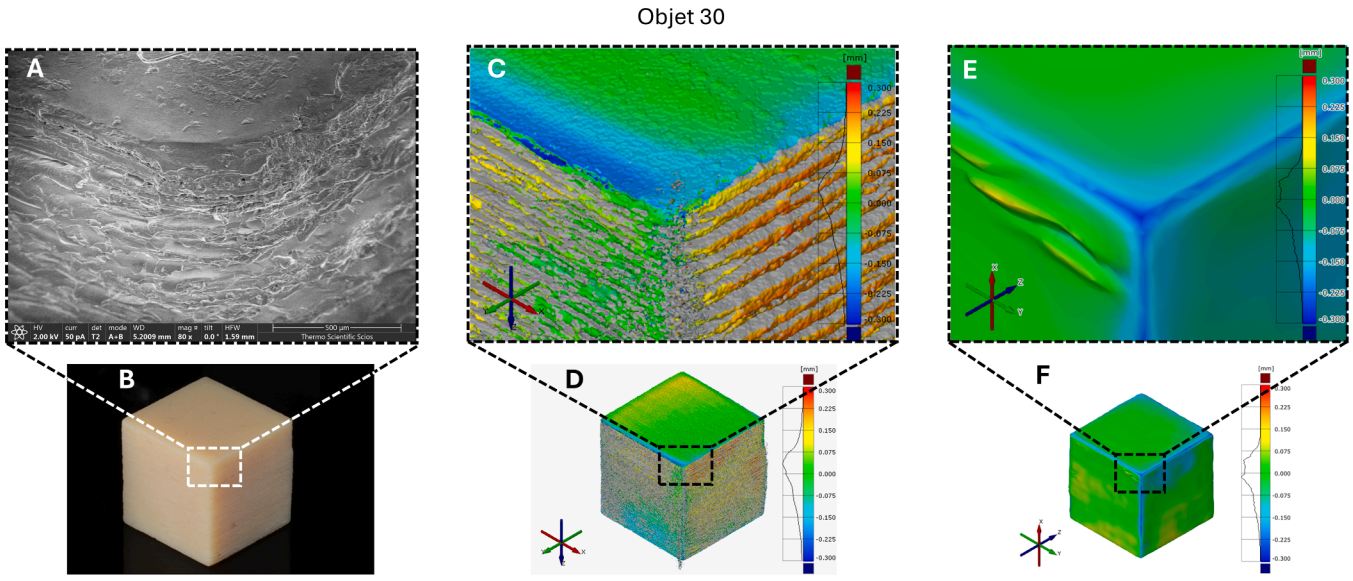

Fig. 6. Analysis of the Objet30 specimen. (A) Scanning electron micrograph (SEM) showing surface topography (original magnification 80 ×). (B) Macroscopic digital photograph of the printed specimen. (D) Color-coded deviation map (GOM Inspect Suite 2020) comparing the reference CAD model against the micro-CT reconstruction. (C) Close-up view of the cube vertex (corner) from the micro-CT comparison. (F) Deviation map comparing the reference CAD model against the optical scan (Atos Core 200). (E) Close-up view of the vertex from the optical scan comparison.

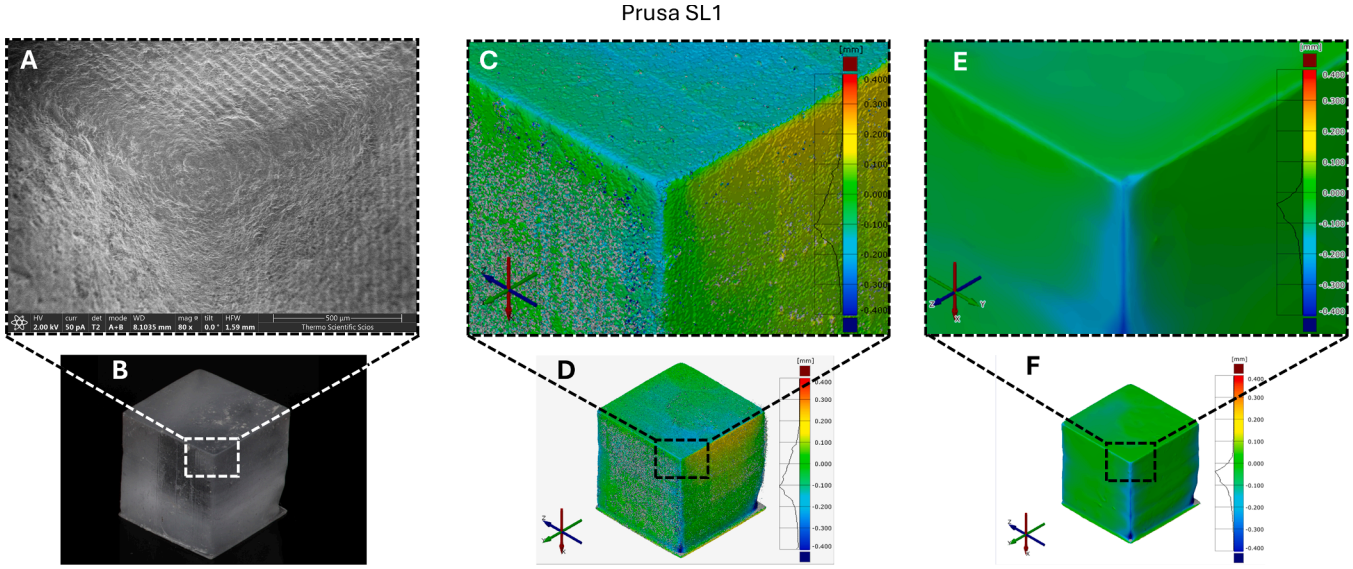

Fig. 7. Analysis of the Prusa SL1 specimen. (A) Scanning electron micrograph (SEM) showing surface topography (original magnification 80 ×). (B) Macroscopic digital photograph of the printed specimen. (D) Color-coded deviation map (GOM Inspect Suite 2020) comparing the reference CAD model against the micro-CT reconstruction. (C) Close-up view of the cube vertex (corner) from the micro-CT comparison. (F) Deviation map comparing the reference CAD model against the optical scan (Atos Core 200). (E) Close-up view of the vertex from the optical scan comparison.

[26]. Similarly, in terms of linear metrology, Saleh et al. reported no clinically significant differences between digital 'on-screen' measurements and those performed manually on physical models, concluding that digital calipers are reproducible tools [27]. However, the accuracy of a model is not defined solely metricfidelity; surface properties are equally critical for clinical applicability [28]. Consequently, to evaluate both dimensional accuracy and surface quality without the limitations of optical resolution, micro-CT represents a superior alternative for the comprehensive quality control of additive manufacturing technologies [29].

Micro-CT imaging relies on the differential attenuation of X-rays as they traverse the specimen, a process governed by the material's specific absorption coefficient. The resulting transmission data generate a series of two-dimensional angular projections, effectively creating a sinogram dataset. For 3D reconstruction, the NRecon software processes these 16-bit TIFF projections in conjunction with geometric parameters extracted from the scan log file. A modified Feldkamp-Davis-Kress (FDK) algorithm - a derivative of the Filtered Back Projection (FBP) method - is then applied. This algorithm utilizes the specific system geometry to accurately transform the 2D angular data into a stack of cross-sectional slices [30].

Micro-CT provides high-resolution three-dimensional imaging capabilities unparalleled by other non-destructive technologies. By applying threshold-based segmentation within CTAn software ('3D Analysis' plug-ins), the volumetric data of the specimen can be precisely isolated from the background. However, significant dimensional

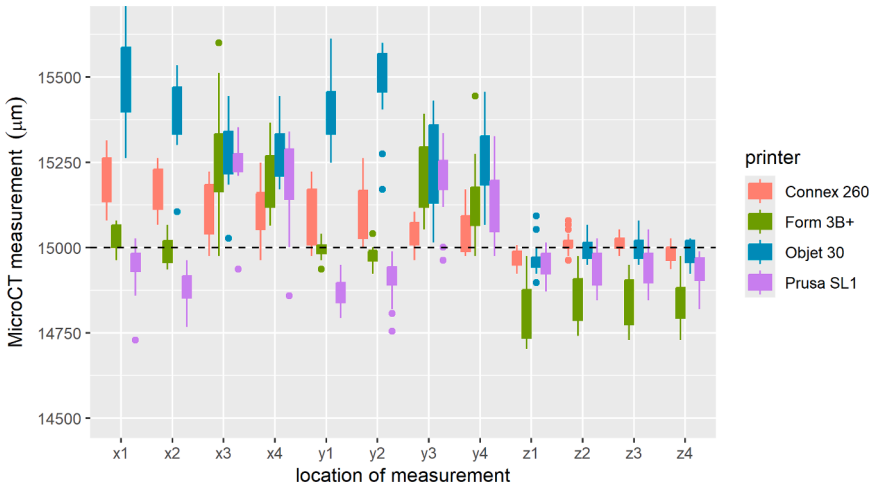

Fig. 8. Boxplots illustrating the dimensional deviations of the measurement methods relative to the micro-CT baseline.

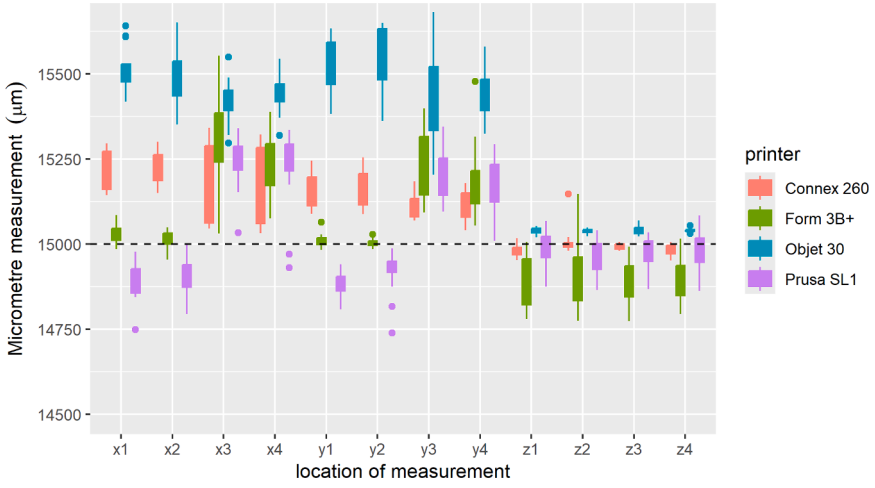

Fig. 9. Boxplots illustrating the dimensional deviations of the measurement methods relative to the digital micrometre baseline.

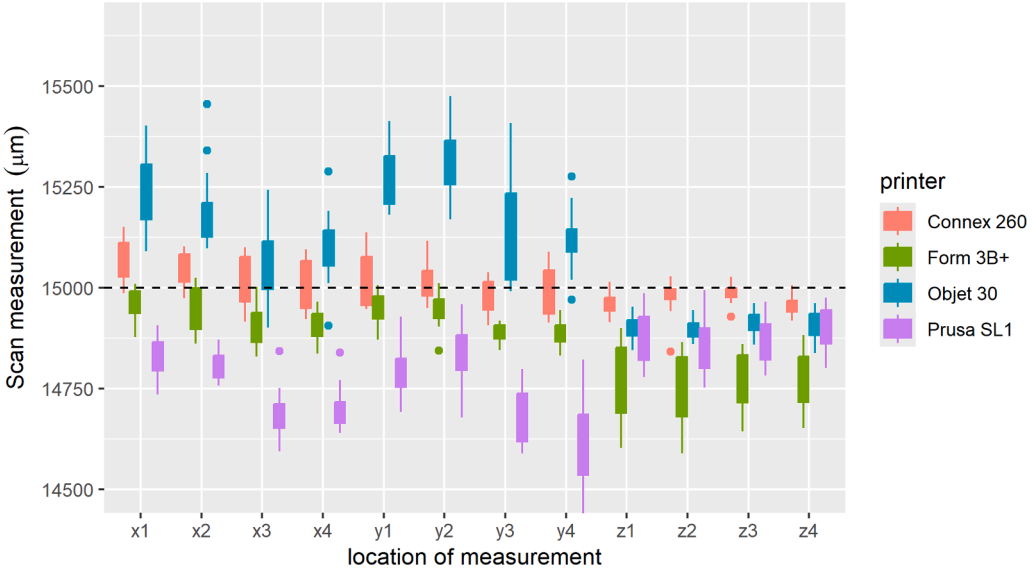

Fig. 10. Boxplots illustrating the dimensional deviations of the measurement methods relative to the optical scan baseline.

deviations have been reported in 3D models fabricated from materials with high atomic numbers, primarily due to the generation of beam-

Table 3
Descriptive statistics for the micro-CT measurements, presenting mean values, standard deviations, and ranges for all X, Y, and Z coordinates across all printer groups.

Printer		X1	X2	X3	X4	Y1	Y2	Y3	Y4	Z1	Z2	Z3	Z4
Connex 260	N	15	15	15	15	15	15	15	15	15	15	15	15
	Mean	15,192.20	15,170.53	15,114.20	15,119.73	15,077.80	15,109.00	15,039.67	15,044.87	14,968.60	15,012.80	15,014.53	14,982.47
	Median	15,184.00	15,171.00	15,132.00	15,158.00	15,041.00	15,093.00	15,054.00	15,028.00	14,976.00	15,002.00	15,015.00	14,976.00
	Std. Dev.	76.73	69.72	81.11	82.82	90.81	87.97	47.23	62.10	28.27	32.77	21.79	26.77
	Minimum	15,080.00	15,067.00	14,976.00	14,963.00	14,976.00	15,002.00	14,963.00	14,976.00	14,924.00	14,963.00	14,976.00	14,937.00
	Maximum	15,314.00	15,262.00	15,223.00	15,249.00	15,223.00	15,262.00	15,106.00	15,171.00	15,008.00	15,080.00	15,054.00	15,028.00
Form 3B+	N	15	15	15	15	15	15	15	15	15	15	15	15
	Mean	15,031.33	14,993.13	15,266.47	15,202.13	14,995.80	14,979.27	15,213.53	15,149.07	14,815.40	14,841.40	14,846.93	14,838.80
	Median	15,041.00	14,989.00	15,301.00	15,171.00	15,002.00	14,989.00	15,22300	15,145.00	14,833.00	14,820.00	14,859.00	14,833.00
	Std. Dev.	38.71	41.33	166.47	102.85	25.84	27.70	108.30	115.09	82.47	75.65	76.78	71.51
	Minimum	14,963.00	14,936.00	14,976.00	15,065.00	14,937.00	14,924.00	15,054.00	14,976.00	14,703.00	14,742.00	14,729.00	14,729.00
	Maximum	15,080.00	15,067.00	15,600.00	15,366.00	15,041.00	15,041.00	15,392.00	15,444.00	14,976.00	14,976.00	14,950.00	14,976.00
Objet 30	N	15	15	15	15	15	15	15	15	15	15	15	15
	Mean	15,493.40	15,411.93	15,278.20	15,286.87	15,402.40	15,490.07	15,240.00	15,256.60	14,968.53	14,992.00	15,005.00	14,988.53
	Median	15,522.00	15,405.00	15,275.00	15,314.00	15,379.00	15,561.00	15,223.00	15,288.00	14,963.00	14,982.00	15,002.00	14,989.00
	Std. Dev.	131.77	142.57	107.92	83.96	105.06	123.92	142.62	109.10	49.80	37.66	44.70	34.25
	Minimum	15,262.00	15,106.00	15,028.00	15,171.00	15,249.00	15,171.00	15,015.00	15,067.00	14,898.00	14,950.00	14,950.00	14,924.00
	Maximum	15,717.00	15,756.00	15,444.00	15,444.00	15,613.00	15,600.00	15,431.00	15,457.00	15,093.00	15,067.00	15,080.00	15,028.00
Prusa SL1	N	15	15	15	15	15	15	15	15	15	15	15	15
	Mean	14,942.20	14,878.00	15,238.60	15,196.47	14,871.13	14,900.60	15,196.73	15,136.33	14,950.00	14,937.87	14,943.93	14,932.67
	Median	14,963.00	14,885.00	15,249.00	15,262.00	14,872.00	14,898.00	15,223.00	15,158.00	14,937.00	14,950.00	14,950.00	14,950.00
	Std. Dev.	73.01	53.94	92.86	142.55	49.74	65.04	102.20	102.56	43.12	61.27	62.51	49.54
	Minimum	14,729.00	14,768.00	14,937.00	14,859.00	14,794.00	14,755.00	14,963.00	14,976.00	14,872.00	14,846.00	14,846.00	14,820.00
	Maximum	15,028.00	14,963.00	15,353.00	15,340.00	14,950.00	14,989.00	15,336.00	15,327.00	15,015.00	15,028.00	15,054.00	14,989.00

Table 4
Micro-CT Measurements vs. Reference Value: analysis of significant differences between mean printed values and the nominal reference value (15,000 μm) across X, Y, and Z coordinates. The magnitude and direction of deviation are included for all statistically significant instances.

Printer	Measurement location	Number of significant cases (out of 4)	Difference
Connex 260	X	4	++
	Y	4	+
	Z	3	+-
Form 3B+	X	3	+++-
	Y	3	++-
	Z	4	–
Objet 30	X	4	+++
	Y	4	+++
	Z	1	+-
Prusa SL1	X	4	++-
	Y	4	++-
	Z	4	-

Key to notation: +: Positive deviations ≤ 120 μm; -: Negative deviations ≤120 μm; +-: Mixed direction, deviations ≤120 μm; ++: Positive deviations ≤250 μm; –: Negative deviations ≤250 μm; ++-: Mixed direction, positive deviations ≤ 250 μm; +++: Positive deviations ≤500 μm; +++-: Mixed direction, positive deviations ≤500 μm.

hardening and metal artifacts [31]. Lorenzo et al. have further validated this reliability for assessing the dimensional features of 3D-printed orthopaedic components [32]. However, the technology is not without constraints. General disadvantages include high operational costs, substantial computational demands, and the requirement for specialized operators and in vitro conditions [28,33]. From our perspective, the strict limitation on specimen size - currently restricted to 25 mm in diameter and 50 mm in length for optimal resolution - is a significant hurdle. Furthermore, the extensive acquisition and reconstruction times far exceed those of conventional diagnostic imaging. Finally, the presence of materials with high atomic numbers can induce beam-hardening and metal artifacts, potentially degrading image quality and distorting volumetric measurements [31]. Despite these challenges, micro-CT remains the most precise and informative method currently available for evaluating dimensional fidelity in dental additive manufacturing. Currently, no industry standard exists for the accuracy of dental AM systems [34]. Németh et al. [4] suggest clinical thresholds of 120 μm for prosthodontics, 250 μm for orthodontics, and up to 500 μm for diagnostic models. Emir & Ayyıldız align with this, citing 100–150 μm as acceptable for fixed prostheses [1]. Kim et al. [36] and Emir & Ayyıldız [1] both identified PolyJet printers as offering superior overall precision compared to SLA. While SLA can achieve high Z-axis resolution - contingent on optimal curing parameters [35] - industrial PolyJet systems have been shown to surpass both SLA and traditional gypsum models in overall accuracy [37].

Multiple studies have highlighted the performance trade-offs between PolyJet and SLA. Emir & Ayyıldız [1] reported that while PolyJet printers generally offered higher overall precision, SLA systems demonstrated superior accuracy specifically in the Z-direction. This Z-axis fidelity in SLA is critical and is governed by the depth of cure, a parameter strictly controlled by irradiance exposure and photoinitiator characteristics [35]. Despite this specific advantage, the broader consensus favors PolyJet for general model fabrication. Kim et al. [36] analysed typodont models using digital linear measurements, concluding that PolyJet exhibited higher precision than SLA. Furthermore, separate investigations have shown that industrial PolyJet systems not only outperform SLA in accuracy but also surpass conventional gypsum casts [37].

In this study, specimens were fabricated using four different 3D printing technologies (SLA, mSLA, PolyJet) and assessed via three metrological techniques. Although statistical analysis revealed significant differences between the micro-CT and micrometre measurements,

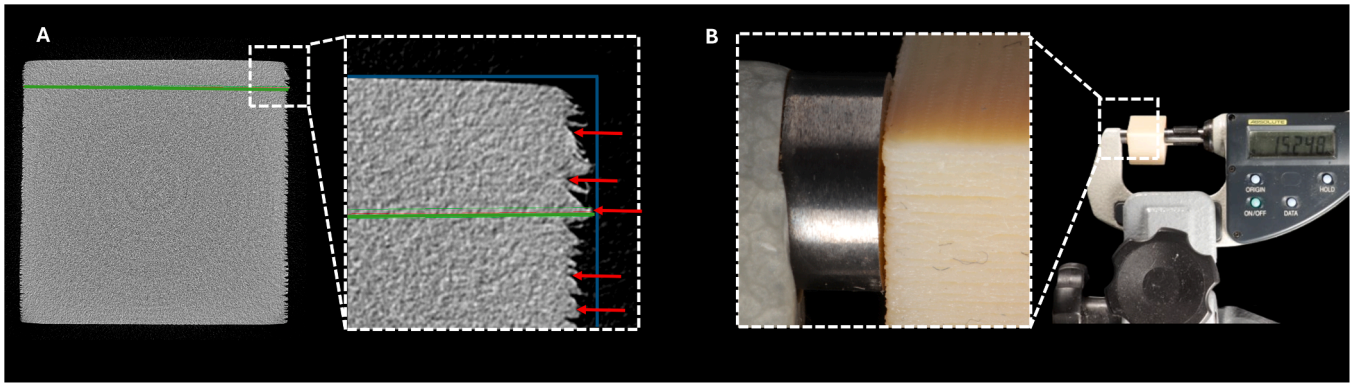

Fig. 11. Comparison of measurement principles. (A) Micro-CT cross-section: The green line represents a typical linear measurement within the slice; red arrows indicate potential variability in selecting start/end points; blue lines denote the external dimensions (distance, surface, edge) accessible to the micrometer. (B) Illustration of a typical contact measurement performed with a micrometer.

the mean discrepancies remained within a narrow interval of –80.5 μm to –22.7 μm. This limited range indicates a high degree of practical concordance between the contact and radiographic methods. Notably, micro-CT demonstrated superior accuracy, attributed to its ability to fit a straight line fitted to the most prominent boundary points within the plane of each CT section. In contrast, the optical scanner consistently produced significantly smaller values across all coordinates, demonstrating a systematic underestimation of the nominal reference value. Consequently, the first null hypothesis was rejected. Collectively, these findings suggest that while the micrometer is reliable for linear dimensions, the micro-CT serves as the superior tool for comprehensive evaluation, capturing both dimensional trueness and surface morphology despite its operational constraints. The specimen dimensions in this study were specifically optimized to accommodate the field-of-view limitations of both micro-CT and SEM imaging.

Significant differences in dimensional distortion were identified across the 3D-printed specimens; consequently, the second null hypothesis was also rejected. This study confirms that dimensional fidelity is influenced by both the chosen additive manufacturing technology and the metrological method.

In accordance with ISO 5725–1:2023, accuracy was evaluated in terms of trueness (closeness to the true result) and precision (repeatability of the result). To isolate the measurement error from the manufacturing error, repeatability was assessed by performing multiple measurements on a single specimen. This protocol ensured that the standard deviation reflected only the variability of the measurement tool, independent of printer performance. The results indicated that optical scanning yielded significantly higher standard deviations (lower precision) across all axes compared to the other methods. Conversely, micro-CT demonstrated superior precision, particularly in two axes where it outperformed the micrometer.

Among the manufacturing systems, the Connex 260 exhibited the highest dimensional fidelity across X, Y, and Z axes, with all printers showing the least distortion along the Z-axis. Ultimately, micro-CT and the micrometer proved to be the most reliable methods for assessing distortions, whereas the optical scanner consistently underestimated dimensions. These findings necessitate caution when relying on optical scanning for high-precision clinical verification.

To enhance the external validity and comparability of future studies, it is imperative that the research community prioritizes the development of standardized test specimens, harmonized measurement protocols, and transparent reporting frameworks. Furthermore, the scope of investigation must expand beyond simple geometric shapes - which is a limitation of this study - to incorporate clinically relevant geometries, larger specimen dimensions, and emerging biocompatible materials. Addressing these gaps is essential for establishing the true clinical applicability of additive manufacturing. Ultimately, such concerted efforts will be the catalyst for translating these technologies into routine dental practice with the requisite accuracy, predictability, and confidence.

5. Conclusions

Within the limitations of the present *in vitro* study, the following conclusions can be drawn:

- Micro-CT offered the highest level of detail concerning the specimen surfaces. The Micro-CT and digital micrometer methods demonstrated superior dimensional trueness compared to the optical scanning protocol, which systematically underestimated dimensions.
- Across all additive manufacturing systems tested, the Z-axis consistently exhibited the lowest magnitude of distortion, indicating higher vertical printing accuracy.
- Among the printer systems evaluated, the Connex 260 (PolyJet) achieved the highest overall dimensional stability, displaying the least distortion in the X, Y, and Z axes.
- Current additive manufacturing technologies retain intrinsic limitations regarding surface smoothness and edge definition, which must be considered during clinical application.

Funding

This research was supported by the Ministry of Culture and Innovation of Hungary through the National Research, Development and Innovation Fund, under grant agreement TKP2021-(TKP2021- EGA funding scheme).

CRediT authorship contribution statement

Márton József Suta: Conceptualization, Investigation, Methodology, Resources, Visualization, Writing – original draft. **Attila Csík:** Investigation, Resources, Validation, Visualization, Writing – review & editing. **Sándor Bodzás:** Methodology, Validation, Writing – review & editing. **Dániel Nemes:** Investigation, Validation, Visualization, Writing – review & editing. **Gábor Balogh:** Validation, Writing – review & editing. **Mónika Béresová:** Investigation, Resources, Validation, Writing – review & editing. **Sándor Manó:** Resources, Validation, Writing – review & editing. **Loránd Csámer:** Investigation, Resources, Validation, Writing – review & editing. **József Mihály Gáll:** Formal analysis, Visualization, Writing – review & editing. **Igor R. Blum:** Investigation, Writing – review & editing. **Csaba Hegedűs:** Conceptualization, Funding acquisition, Investigation, Methodology, Project administration, Resources, Supervision, Visualization, Writing – original draft, Writing – review & editing.

Declaration of competing interest

IRB is an Editorial Board Member of Journal of Dentistry. Given his role in Journal of Dentistry, IRB had no involvement in the peer review of this article and has no access to information regarding its peer review. The authors declare that they have no other known competing financial interests or personal relationships that could have appeared to influence the work reported in this paper.

Acknowledgements

None.

Data availability

The data supporting the findings of this study are available from the corresponding author upon request.

References

[1] F. Emir, S. Ayyildiz, Accuracy evaluation of complete-arch models manufactured by three different 3D printing technologies: a three-dimensional analysis, J. Prosthodont. Res. 65 (2021) 365–370, https://doi.org/10.2186/jpr.JPOR_2019_579.
[2] Y. Tian, C. Chen, X. Xu, J. Wang, X. Hou, K. Li, X. Lu, H. Shi, E.-S. Lee, H.B. Jiang, A review of 3D printing in dentistry: technologies, affecting factors, and applications, Scanning 2021 (2021) 1–19, https://doi.org/10.1155/2021/9950131.
[3] A. Zandinejad, F. Floriani, W.S. Lin, A. Naimi-Akbar, Clinical outcomes of milled, 3D-printed, and conventional complete dentures in edentulous patients: a systematic review and meta-analysis, J. Prosthodont. 33 (2024) 736–747, https://doi.org/10.1111/jopr.13859.
[4] A. Németh, V. Vitai, M.L. Czumbel, B. Szabó, G. Varga, B. Kerémi, P. Hegyi, P. Hermann, J. Borbély, Clear guidance to select the most accurate technologies for 3D printing dental models – a network meta-analysis☆, J. Dent. 134 (2023) 104532 https://doi.org/10.1016/j.jdent.2023.104532.
[5] A.E. Alexander, N. Wake, L. Chepelev, P. Brantner, J. Ryan, K.C. Wang, A guideline for 3D printing terminology in biomedical research utilizing ISO/ASTM standards, 3D Print, Med. 7 (2021) 8, https://doi.org/10.1186/s41205-021-00098-5.
[6] B. Morón-Conejo, J. López-Vilagran, D. Cáceres, S. Berrendero, G. Pradíes, Accuracy of five different 3D printing workflows for dental models comparing industrial and dental desktop printers, Clin. Oral Investig. 27 (2022) 2521–2532, https://doi.org/10.1007/s00784-022-04809-y.
[7] E. Caussin, C. Moussally, S. Le Goff, T. Fasham, M. Troizier-Cheyne, L. Tapie, E. Dursun, J.-P. Attal, P. François, Vat photopolymerization 3D printing in dentistry: a comprehensive review of actual popular technologies, Materials (Basel) 17 (2024) 950, https://doi.org/10.3390/ma17040950.
[8] T.D. Ngo, A. Kashani, G. Imbalzano, K.T.Q. Nguyen, D. Hui, Additive manufacturing (3D printing): a review of materials, methods, applications and challenges, Compos. Part B Eng. 143 (2018) 172–196, https://doi.org/10.1016/j.compositesb.2018.02.012.
[9] H.B. Mamo, M. Adamiak, A. Kunwar, 3D printed biomedical devices and their applications: a review on state-of-the-art technologies, existing challenges, and future perspectives, J. Mech. Behav. Biomed. Mater. 143 (2023) 105930, https://doi.org/10.1016/j.jmbbm.2023.105930.
[10] A. Kessler, R. Hickel, M. Reymus, 3D Printing in dentistry—State of the art, Oper. Dent. 45 (2020) 30–40, https://doi.org/10.2341/18-229-L.
[11] S.C. Ligon, R. Liska, J. Stampfl, M. Gurr, R. Mülhaupt, Polymers for 3D printing and customized additive manufacturing, Chem. Rev. 117 (2017) 10212–10290, https://doi.org/10.1021/acs.chemrev.7b00074.
[12] G. Budzik, J. Woźniak, A. Paszkiewicz, Ł. Przeszłowski, T. Dziubek, M. Dębski, Methodology for the quality control process of additive manufacturing products made of polymer materials, Materials (Basel) 14 (2021) 2202, https://doi.org/10.3390/ma14092202.
[13] E. Anadioti, B. Kane, Y. Zhang, M. Bergler, F. Mante, M.B. Blatz, Accuracy of dental and industrial 3D printers, J. Prosthodont 31 (2022) 30–37, https://doi.org/10.1111/jopr.13470.
[14] D.C. Chan, A.K. Chung, J. Haines, E.H. Yau, C.C. Kuo, The accuracy of optical scanning: influence of convergence and die preparation, Oper. Dent. 35 (2011) 486–491, https://doi.org/10.2341/10-067-L.
[15] C. Bindhu Sree, P. Koka, I.K. Sri, J.A. Alex, K.D. Rani, V.B. Chander, Comparative evaluation of trueness of dental impressions using digital scanners: an In vitro study, J. Pharm. Bioallied. Sci. 17 (2025) S789–S791, https://doi.org/10.4103/jpbs.jpbs_615_25.
[16] H. Wickham, ggplot2 elegant graphics for data analysis, second ed., Springer international publishing, Cham (2016), https://doi.org/10.1007/978-3-319-24277-4.
[17] Stratasys Support Center, Design for additive manufacturing with PolyJet. https://support.stratasys.com/SupportCenter/HTML5UserGuides/Design_DFAM_Guide_July_2020/Responsive.HTML5/index.html#t=DOC-01103_x_Design-PJ-AM-Guide-HTML%2FDfAM_Guide-Chapter%2FDfAM_Guide-Chapter.htm&rhsearch=author, 2020 accessed 31 March 2025.
[18] Formlabs, Form 3 design guide. https://3dformlabs.com/rs/060-UIG-504/images/WP-EN-Form-3-Design-Guide.pdf?mkt_tok=MDYwLVVJRy01MDQAAAGXP54j5zSaPsSVYI6DBR0FH1gJrgJrVhBq6xdr5vNNoc4LWOI7IqhnQ5r80XDbz-e8_BOOtao9gU_ifOW9qO1gQHScZDJA6xq8chDAwhGt-WByjdI, 2020 accessed 31 March 2025.
[19] A. Nulty, A comparison of trueness and precision of 12 3D printers used in dentistry, BDJ Open 8 (2022) 14, https://doi.org/10.1038/s41405-022-00108-6.
[20] F.G. Mangano, O. Admakin, M. Bonacina, F. Biaggini, D. Farronato, H. Lerner, Accuracy of 6 desktop 3D printers in dentistry: a comparative In vitro study, Eur. J. Prosthodont. Restor. Dent. 28 (2020) 75–78, https://doi.org/10.1922/EJPRD_2050Mangano11.
[21] M. Braian, R. Jimbo, A. Wennerberg, Production tolerance of additive manufactured polymeric objects for clinical applications, Dent. Mater. 32 (2016) 853–861, https://doi.org/10.1016/j.dental.2016.03.020.
[22] A. Unkovskiy, P.H.-B. Bui, C. Schille, J. Geis-Gerstorfer, F. Huettig, S. Spintzyk, Objects build orientation, positioning, and curing influence dimensional accuracy and flexural properties of stereolithographically printed resin, Dent. Mater. 34 (2018) e324–e333, https://doi.org/10.1016/j.dental.2018.09.011.
[23] C. Johansson, J. Dibes, L.E.L. Rodriguez, E. Papia, Accuracy of 3D printed polymers intended for models and surgical guides printed with two different 3D printers, Dent. Mater. J. 40 (2021) 339–347, https://doi.org/10.4012/dmj.2020-039.
[24] H.B. Lee, M.J. Noh, E.J. Bae, W.S. Lee, J.H. Kim, Accuracy of zirconia crown manufactured using stereolithography and digital light processing, J. Dent. 141 (2024) 104834, https://doi.org/10.1016/j.jdent.2024.104834.
[25] S. Song, J. Zhang, M. Liu, F. Li, S. Bai, Effect of build orientation and layer thickness on manufacturing accuracy, printing time, and material consumption of 3D printed complete denture bases, J. Dent. 130 (2023) 104435, https://doi.org/10.1016/j.jdent.2023.104435.
[26] Q. Wan, R. Daher, H. Lee, H.B. Kwon, J.S. Han, J.H. Lee, Reliability of digital repeated-scan superimposition and single-scan techniques for wear volume loss assessment on flat surfaces, J. Dent. 138 (2023) 104738, https://doi.org/10.1016/j.jdent.2023.104738.
[27] W.K. Saleh, E. Ariffin, M. Sherriff, D. Bister, Accuracy and reproducibility of linear measurements of resin, plaster, digital and printed study-models, J. Orthod. 42 (2015) 301–306, https://doi.org/10.1179/1465313315Y.0000000016.
[28] H. Eliasova, T. Dostalova, M. Jelinek, J. Remsa, P. Bradna, A. Prochazka, M. Kloubcova, Surface morphology of three-dimensionally printed replicas of upper dental arches, Appl. Sci. 10 (2020), https://doi.org/10.3390/app10165708.
[29] A. du Plessis, I. Yadroitsev, I. Yadroitsava, S.G. Le Roux, X-ray microcomputed tomography in Additive manufacturing: a review of the current technology and applications, 3D print, Addit. Manuf. 5 (2018) 227–247, https://doi.org/10.1089/3dp.2018.0060.
[30] Bruker, Method note an overview of NRecon: reconstructing the best images from your microCT scan. https://www.foa.unesp.br/Home/pesquisa/escritoriodeapoioapesquisa/mn062_nrecon-overview.pdf?t&utm_source=perplexity, 2014 accessed 31 March 2025.
[31] J. Fang, D. Zhang, C. Wilcox, B. Heidinger, V. Raptopoulos, A. Brook, O.R. Brook, Metal implants on CT: comparison of iterative reconstruction algorithms for reduction of metal artifacts with single energy and spectral CT scanning in a phantom model, Abdom. Radiol. 42 (2017) 742–748, https://doi.org/10.1007/s00261-016-1023-1.
[32] L. Dall'Ava, H. Hothi, J. Henckel, A. Di Laura, S. Bergiers, P. Shearing, A. Hart, Dimensional analysis of 3D-printed acetabular cups for hip arthroplasty using X-ray microcomputed tomography, Rapid Prototyp, J. 26 (2020) 567–576, https://doi.org/10.1108/RPJ-06-2019-0175.
[33] T. Kulczyk, M. Rychlik, D. Lorkiewicz-Muszyńska, M. Abreu-Głowacka, A. Czajka-Jakubowska, A. Przystańska, Computed tomography versus optical scanning: a comparison of different methods of 3D data acquisition for tooth replication, Biomed Res. Int. 2019 (2019) 1–7, https://doi.org/10.1155/2019/4985121.
[34] M. Braian, R. Jimbo, A. Wennerberg, Production tolerance of additive manufactured polymeric objects for clinical applications, Dent. Mater. 32 (2016) 853–861, https://doi.org/10.1016/j.dental.2016.03.020.
[35] J.W. Stansbury, M.J. Idacavage, 3D printing with polymers: challenges among expanding options and opportunities, Dent. Mater. 32 (2016) 54–64, https://doi.org/10.1016/j.dental.2015.09.018.
[36] S.Y. Kim, Y.S. Shin, H.D. Jung, C.J. Hwang, H.S. Baik, J.Y. Cha, Precision and trueness of dental models manufactured with different 3-dimensional printing techniques, Am. J. Orthod. Dentofac. Orthop. 153 (2018) 144–153, https://doi.org/10.1016/j.ajodo.2017.05.025.
[37] M. Buda, M. Bratos, J.A. Sorensen, Accuracy of 3-dimensional computer-aided manufactured single-tooth implant definitive casts, J. Prosthet. Dent. 120 (2018) 913–918, https://doi.org/10.1016/j.prosdent.2018.02.011.